Mansoura Journal of Chemistry, vol. 34(2), December 2007

TEXTURAL PROPERTIES OF LAYERED DOUBLE HYDROXIDES: EFFECT OF SUBSTITUTION OF MAGNESIUM BY COPPER OR IRON

L. Saad
Egyptian Petroleum Research Institute- Refining Division
Hai Elzohoor-Nasr City- Cairo- Egypt. Postal code: 11727
(Received: 16 / 10 / 2007)

ABSTRACT

Layered double hydroxides (LDHs) in which magnesium was partially substituted by copper or iron, were prepared by a co precipitation method. The prepared materials were characterized by X-ray diffraction, EDX, FT-IR spectroscopy. N2-adsorption, scanning electron microscopy (SEM) and transmission electron microscopy (TEM).The substituted sample preserved the hydrotalcite layered structure though their textural properties underwent important modifications. Copper substituted LDH emphasized higher contribution of mesoporous characteristic. For iron substituted-LDH the mesopores were enlarged and constriction in the porous structure was accentuated. Microscopic morphology characteristics contributed to establish the textural properties of the samples.

Keywords: Hydrotalcites; Texture properties; Mesoporosity; Microporosity; Microscopic morphology

INTRODUCTION

Layered double hydroxides (LDHs). also known as hydrotalcite like compounds or simply hydrotalcites (HT) are bi-dimensional layered materials with the general formula $[M^{2+}_{1-x} M^{3+}_{x} (OH)^{x+}_{2} (A^{n-}_{x/n})^{x-}.m\ H_2O]$ where. M^{2+} is a divalent cation (Mg^{2+}, Co^{2+}, Ni^{2+}, Zn^{2+}, Mn^{2+}, Cd^{2+}). M^{3+} is a trivalent cation (Al^{3+}, Fe^{3+}, Cr^{3+}, Ga^{3+}) and A^{n-} is an anion

Corresponding author. L. Saad
Fax: +2022747433 E-mail address: lamiakaid@yahoo.com

[Cavani, et al. (1991); de Roy, et al. (1992); Rives & Ulibarri (1999); Triforo & Vaccari (1996); Khan &Hare (2002) and Vichi & Alves (1997)]. These solids present a brucite like structure, where metallic cations are located in the center of an edge-sharing octahedral network. Isomorphous substitution of divalent cations by trivalent ones generates positive charges on the layers, which are compensated by anions located in the interlayer region. Water molecules are arranged in a liquid-like configuration (for schematic view of hydrotalcite structure (see Ref. **[Cavani, et al. (1991])** **[Cavani, et al. (1991); de Roy, et al. (1992); Rives & Ulibarri (1999) and Triforo & Vaccari (1996)]**.

Hydrotalcites have received considerable attention in recent decades due to their potential applications in many different fields, such as ion exchangers, adsorbents, medical science and catalysts **[Lazaridis, et al. (2004); Vaccari, (1999); Figueras, (2004) and Khan & Lei (2001)]**. This wide range of applications comes from some special features of the hydrotalcite structure, as follows: possibility of accommodation of cations of different natures in the sheets, atomic scale homogeneity, and possibility of intercalation of several types of anions (inorganic, organic, organometallic, polyoxometalates) and formation of mixed oxides under thermal treatment **[Rives & Ulibarri (1999) and Khan & Hare (2002)]**. It is also known that hydrotalcites containing transition metals tend to exhibit enhanced catalytic activity owing to the presence of redox and Lewis sites that may be combined with structural and geometric features to yield solid with the desired properties.

In defining or tailoring the catalytic and adsorption properties, the crystallinity and textural characteristics of LDH are of particular importance. For example, the shape and the size of pores associated with the uniformity of the porous structure can promote shape selectivity; a high surface area will facilitate guest-host interactions.

In order to get information about the possibility to tailor textual properties of LDH, the aim of this study is to prepare Mg Al-LDH, Mg Cu Al-LDH and Mg Fe Al-LDH and also to investigate how the textural properties can be altered through direct synthesis when magnesium is partially substituted by either copper or iron. The effects of magnesium substitution by copper or iron on the textural properties and morphology of the materials are reported.

2. EXPERIMENTAL

All the samples were prepared by co precipitation method at 65°C and constant pH under bubbling constant flow of nitrogen in the reaction medium and vigorous stirring. After an aging step, the precipitates were separated via centrifugation, washed extensively with distilled warm water until sodium free and then dried at 65°C **[Miyata, (1983)]**.

2.1. Mg Al-LDH

Two aqueous solutions were required; the first one containing 0.9 mol/l $MgSO_4.7H_2O$ and 0.3mol/l $Al_2(SO_4)_3.18H_2O$ (for a ratio Mg/Al=3) and the second one, 3 mol/l of NaOH and 0.8mol/l Na_2CO_3 (CO_3^{-2}/Al^{3+} + Mg = 0.67, OH^-/Al^{3+} + Mg = 2.5) were introduced into a flask by two dosing pumps and mixed under vigorous stirring, at a constant temperature 65°C and constant pH of 9.5. The resulting white precipitate was aged at this temperature for 18h with stirring. The precipitate was washed extensively with warm distilled water until sodium free and then dried at 65°C.

2.1.2 Mg Cu Al-LDH

An aqueous solution of $MgSO_4.7H_2O$ (0.75 mol/l)/ $Al_2(SO_4)_3.18H_2O$ (0.3mol/l)/ $Cu(NO_3)_2.6H2O$ (0.15mol/l) and an aqueous solution of NaOH/ Na_2CO3 were added drop wise together over a period of 2h at a constant pH value of 8.5. The resulting light blue precipitate was aged at 65°C for 18h under stirring.

2.1.3. Mg Fe Al- LDH

An aqueous solution of $MgSO_4.7H_2O$ (0.75 mole/l)/ $Al_2(SO_4)_3$ (0.3 mol/l)/ Fe SO_4 (0.15 mol/l) and an aqueous solution of $NaOH/Na_2CO_3$ were added drop wise together over 2h period at a constant pH of 8.5. The resulting orange precipitates were aged at for 18h under stirring 65°C.

2.2. Materials characterization

The structures of the prepared materials were studied by EDX, XRD, FT-IR, TG-DTA, N_2-adsorption, SEM & TEM methods. Powder X-ray diffraction (XRD) measurement was performed with a XD-D1-X-ray diffraction Shimadzu apparatus, equipped with a monochromator for the CuKα radiation operating at 40 KV over a 2Θ rang from 4° to 60°. The

diffraction patterns were identified by comparing with those included in JCPDS (Joint Committee of Powder Diffraction Standards) database. The apparatus provided with software program to study the changes in crystallites size of the synthesized materials.

IR spectra were recorded on Shimadzu FTIR spectrometer under the following conditions: 200 scans in the mid-IR range (400-4000cm^{-1}) using KBr (ratio 5/95 wt.%) pellets, and resolution of 4 cm^{-1}.

TG-DTA was recorded under air with Shimadzu TGA-50 and DTA-50 analyzer using 10 mg of sample and a rate 10 $Kmin^{-1}$.

N_2 adsorption-desorption measurements conducted at -196°C using Quanta Chrome Nova 2000 instrument. Prior to the measurements the samples were heated for 3 h under vacuum at 200°C in order to expel the interlayer water molecules.

The BET specific surface area (S_{BET}) was calculated by using the standard Brunauer, Emmett and Teller method on the basis of adsorption data. The pore size distributions (PSD) were calculated from both adsorption desorption branches of the isotherm using the Barret, Joyner and Halenda method (BJH) **[Gregg & Sing (1982)]**. For SEM a Hitachi S-800 scanning microscope (SEM) was utilized for the investigation of microscopic morphologies. Transmission electron microscopy (TEM) analysis was performed on a Hitachi instrument operating at 200KV. The samples were prepared by dispersing powders in ethanol.

3. RESULTS AND DISCUSSION

3.1. Structural characteristics

3.1.1. XRD and EDX analysis

The chemical compositions, lattice parameters, interlayer free spacing and crystallite size of the prepared samples are presented in Table 1. The Mg/Cu/Al and Mg/Fe/Al atomic ratios determined by EDX are coincident with those of the starting mixed aqueous solutions within the experimental errors. The EDX results reveal that only magnesium was substituted by copper or iron during the preparation procedure.

The diffraction patterns for all samples (Fig. 1) exhibit sharp intense peaks close to $2\Theta = 11°$, 24°, 35°, 60° and 62° ascribed to diffraction by basal planes (003), (006), (012), (110) and (113) . These diffractions are recorded at ca 7.8, 3.87 and 2.6 Å, very close to those reported in literature for hydrotalcite-like material containing interlayer carbonate anions (JCPDS: 41-1428). **[Cavani, et al. (1991)]**.

Table (1): Chemical composition and lattice parameters of MgAl- LDH and M- LDHs.

Sample	Atomic ratio from EDX					Lattice parameters			IFS (Å)	Crystallite size (nm)
	O	Mg	Al	Cu	Fe	a	c	d_{003}		
MgAl-LDH	76	16.8	6	____	____	3.1	23.3	7.8	3	3.41
Fe-LDH	74.4	13.8	6.4	____	5.51	3.1	23.1	7.7	2.9	12.1
Cu-LDH	72.2	14	6.6	5.1		3.1	23	7.65	2.8	3.8

IFS: inter layer free spacing.
M: Copper or iron

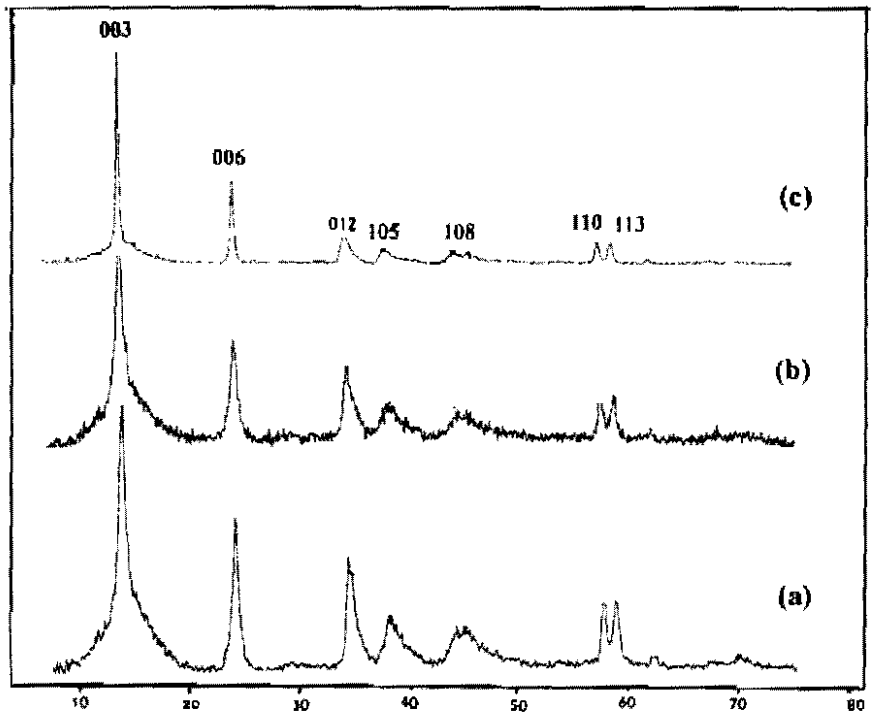

Fig. (1): X-ray diffraction patterns of (a) Mg Al-LDH ; (b) Cu-LDH; (c) Fe-LDH.

The d-spacing for planes (003) for a hexagonal packing (rhombohedral R-3m) is in the range of 7.8 -7.68 Å for all samples. Assuming a value of 4.8Å for the width of brucite layer **[Cavani, et al. (1991)]**, the interlayer free space value (***IFS***) are calculated by subtracting the thickness of LDH layer (4.8Å) from the calculated $d_{(003)}$ spacing **[Kannan, et al. (2005)]**. The decrement in IFS values from 3Å for Mg Al LDH to 2.9 Å for Fe LDH and 2.80Å for Cu LDH; suggests a distortion of LDH net work which induced in the process of isomorphous substitution of magnesium by either copper or iron due to Jahn-Teller distortion which leads to poor long- range ordering **[Iglesias, et al. (2005)]**.

The lattice parameters were calculated for a hexagonal cell on the basis of rhombohedral R-3m symmetry (Table 1). The thickness of the brucite- like layer is almost constant for most hydrotalcites synthesized of first series transition cations, as it mainly depends on the ionic radii of the cations existing in the layers and of the hydroxyl group, and so basal plane spacing depends mostly on the nature and orientation of interlayer anions **[Cavani, et al. (1991)]**.

Parameter **a** corresponds to the average closest cation-cation distance within the brucite-like layer, it has been calculated as $a=2\,d_{(110)}$, the peak corresponding to diffraction by planes (110) being the first of the doublet recorded at 2θ *ca* $60°$ **[Crivello, et al. (2005)]**, while the parameter **c** is calculated from the position of the first, intense basal peak (*plane 003 if hexagonal packing is assumed*) and $c = 3d_{(003)}$ **[Crivello, et al. (2005) and Trujillano, et al. (2005)]**.

No significant positional changes in the basal reflections or lattice parameter (***a***) were noted for the substituted samples. This may be due to the correspondence subtle differences in the octahedral ionic radii of Cu^{2+} (0.73Å) and Mg^{+2} (0.72Å) **[de Roy, et al. (1992)]**. However, the smaller ionic radius Fe^{2+} (0.61Å) is suggested to incorporate into the burcite- like structure through dispersion between the sheets.

The decrease of parameter ***c*** and the d_{003} (basal spacing calculated from the 003 reflection in XRD pattern) can be attributed to the modified electrostatic interactions between the layer and the interlayer network when another metal is introduced in the LDH layer **[Velu, et al. (1999)]**.

Thus, EDX results, together with the structural changes that are revealed by XRD, demonstrate the incorporation of iron and copper in the LDH network.

3.1.2. FT-IR Spectroscopy

The FT-IR spectra of the synthesized samples are included in Fig. 2. For all samples IR spectra are quite similar though some differences can be noticed in the intensity and the broadness of the bands. All the spectra are characteristic of hydrotalcite-like structure with CO_3^{2-} as interlayer anion **[Cavani, et al. (1991)]**. The broad band around 3500 cm^{-1} is due to OH- stretching mode of hydrogen-bonded hydroxyl groups and of water molecules. This broad band includes a broad shoulder close to 3000 cm^{-1} which has been ascribed to the OH stretching mode of hydroxyl groups hydrogen bonded to interlayer carbonate anions **[Labajos, et al. (1992)]**.

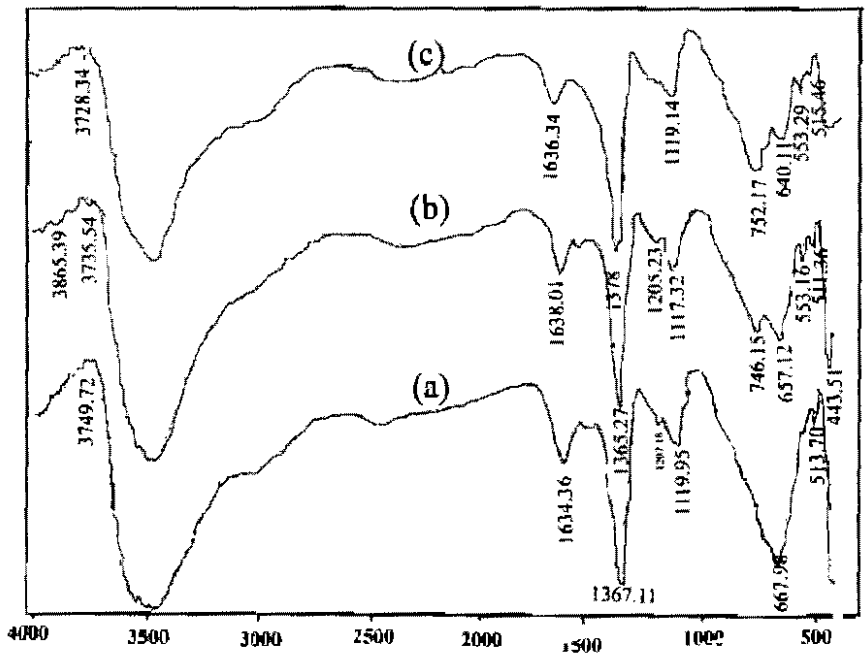

Fig. (2): FT-IR spectra of (a) Mg AL-LDH; (b) Cu-LDH; (c) Fe-LDH.

The narrower adsorption close to 1367 cm^{-1} is attributed to the υ_3 vibration mode of interlayer carbonate species **[Hernandes-Moreno, et al. (1985)]**. The shift of this band for Cu- LDH (1365 cm^{-1}) and Fe- LDH (1378 cm^{-1}) is suggested to be related to the restricted symmetry in the interlayer space which actually resulted from the distortion of LDH

network accompanying the isomorphous substitution by Cu^{2+} or Fe^{2+} respectively. The band at 1636 cm^{-1} is assigned to the bending mode of interlayer water **[Serna, et al. (1977)]**. The band appears close to 1119 cm^{-1} is due to the vibration mode of SO_4^{2-} anion that still exists in the interlayer. .The bands appear between 640-667 and 746-752 Cm^{-1} respectively are ascribed to υ_4 and respective υ_2 vibration modes of CO_3^{2-} anion **[Miyata & Okada (1977)]**.

We can remark some differences in the intensities of these bands between Mg Al- LDH and the substituted samples; may ascribed the orientation of CO_3^{2-} in the interlayer as a consequence of different electrostatic forces that act in the network of substituted samples.

For all sample spectra, weak bands at lower wave number are more probably due to vibration implying M-O, MO-M and O-M-O bonds in the layers corresponding to the hydrotalcite lattice vibrations **[Miyata, (1975) and Aramendia, et al. (1999)]**.

3.1.3. Thermal analysis

Representative thermal analysis profiles (TGA &DTA) for the synthesized samples are shown in Fig. 3.

TGA Profiles exhibit three well defined weight losses which are complemented by three endothermic peaks in the DTA curves (Fig.3). These weight losses can be attributed to the following thermal events,

(i) release of physically adsorbed, (ii) release of interlayer water (represented by two endothermic peaks at 100& 220°C respectively) and. (iii) removal of water through condensation of layer hydroxyl groups and also the decomposition of counter anions from interlayer as CO_2 (indicated by endotherms at 380-430°C) **[Velu & Swamy (1996)]**.

The weight loss in the first two stages is higher for Cu-LDH (24wt. %) than for Fe- LDH (15 wt. %) or Mg Al-LDH (13 wt.%).The weigh loss at the third stage decreases to 6% for Cu-LDH and ~ 10% for Fe-LDH and Mg Al-LDH. Therefore, the total weight loss increases by 10% for Cu LDHS and to 5% for Fe- LDH revealing a different behavior of substituted samples.

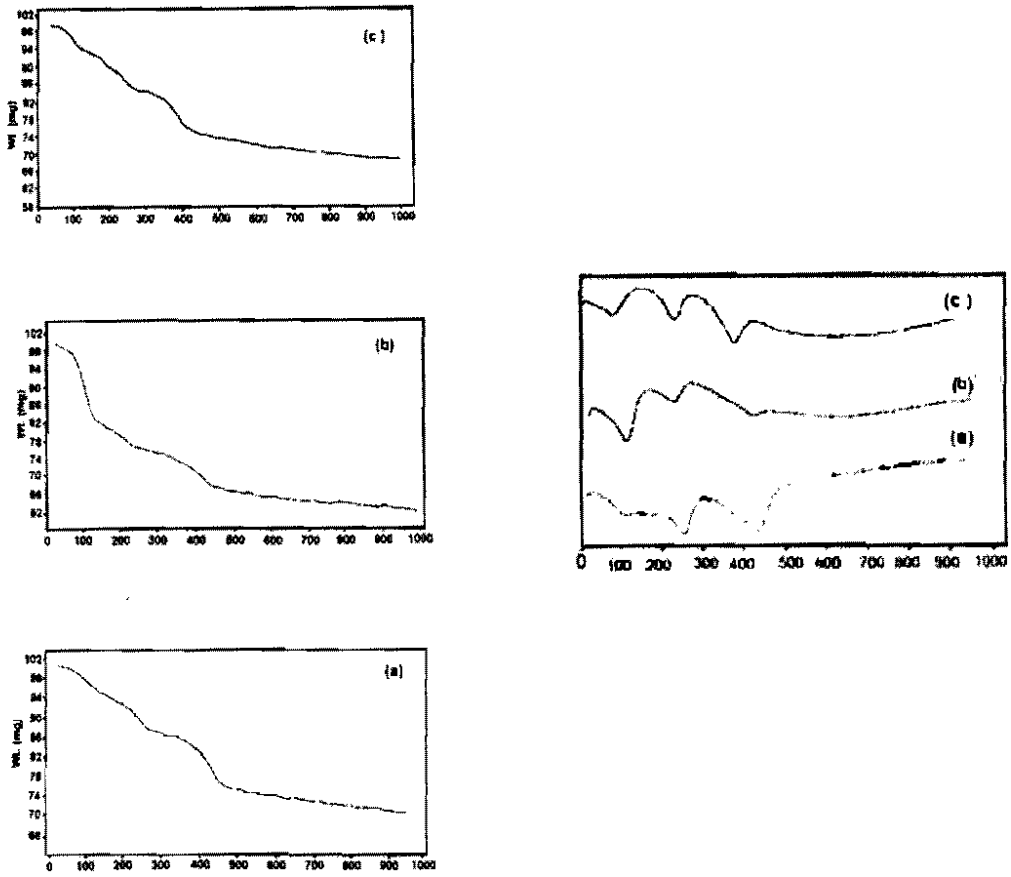

Fig. (3): TGA & DTA of (a) Mg Al-LDH; (b) Cu-LDH; (c) Fe-LDH

The DTA profiles are qualitatively similar for all synthesized samples, differing only in the intensity and temperature where the minimum of the third peak occur. The broadening of the third endothermic peak for Cu LDHs (at 400°C) , while, it appears more sharper at 430°C for Mg Al-LDH is indeed expected , since magnesium is better stabilized in an octahedral coordination of hydrotalcite like lattice structure than copper ,which is inherently less stable in octahedral coordination because of tetragonal Jahn Teller distortion **[Kannan, et al. (2005)]**.

In addition, the dispersion of tiny Fe^{+2} (0.61Å) between the LDH sheets leads to a reduction in the thermal stability of the hydrotalcite structure owing to the possibility of oxidation of these cations **[Rives, et al. (2001)]**.

Thus, in agreement with the previously reported results of Kannah and Swamy **[Kannan & Swamy (1997)]**, the modified electronic interaction between the ions of hydrotalcite-like network when new cations incorporated into the network is expected to be responsible for the difference in the behavior of the substituted samples.

3.2.3 Textural characteristics

All synthesized samples display type II nitrogen adsorption isotherm according to IUPC classification **[Sing, et al. (1985)]**. The curves (Fig.4a) show a rather small hysteresis loop (type H_3) closing at relative pressure around 0.6 for all three samples, indicating similar pore architecture of mesoporous dimensions. The mesoporosity is further confirmed from t-plots (Fig.4b) which show in all samples an upward deviation that is more clearly observed in Cu-LDH and Fe-LDH respectively.

The specific surface area decreases significantly for Cu & Fe substituted samples respectively, Cu- LDH sample reveal almost the same mean pore diameter as the Mg AL- LDH sample, while, the pore diameter for Fe- LDH sample drastically increases. This may indicates the interstitial substitution of Mg^{+2} by Cu^{+2}, while, the highly dispersed tiny Fe^{+2} (0.61Å) is expected to be responsible for the creation of wider pores. Furthermore, the observed decrease in the total pore volume for Cu- LDH is expected to be due the blocking of some pores by copper species.

The S_{BET} values, the total pore volume (V_p) and the mean pore diameter (D_p) are summarized in Table 2.

In agreement with the crystallite size measurements (Table1), Fe-LDH reveals the largest crystallite size (12.1 nm) which may results from agglomeration of the highly dispersed tiny Fe^{+2} species which probably interconnected with burcite-like network cations in a manner gives rise to large crystals with wider interparticle space (D_p=21.2 nm). Furthermore , the subtle difference in the octahedral ionic radii of Mg^{+2} (.72 Å) and Cu^{+2} (.73 Å) may explain the same pore dimensions and crystallite sizes for both Mg Al-LDH and Cu-LDH which may indicates the interstitial substitution.

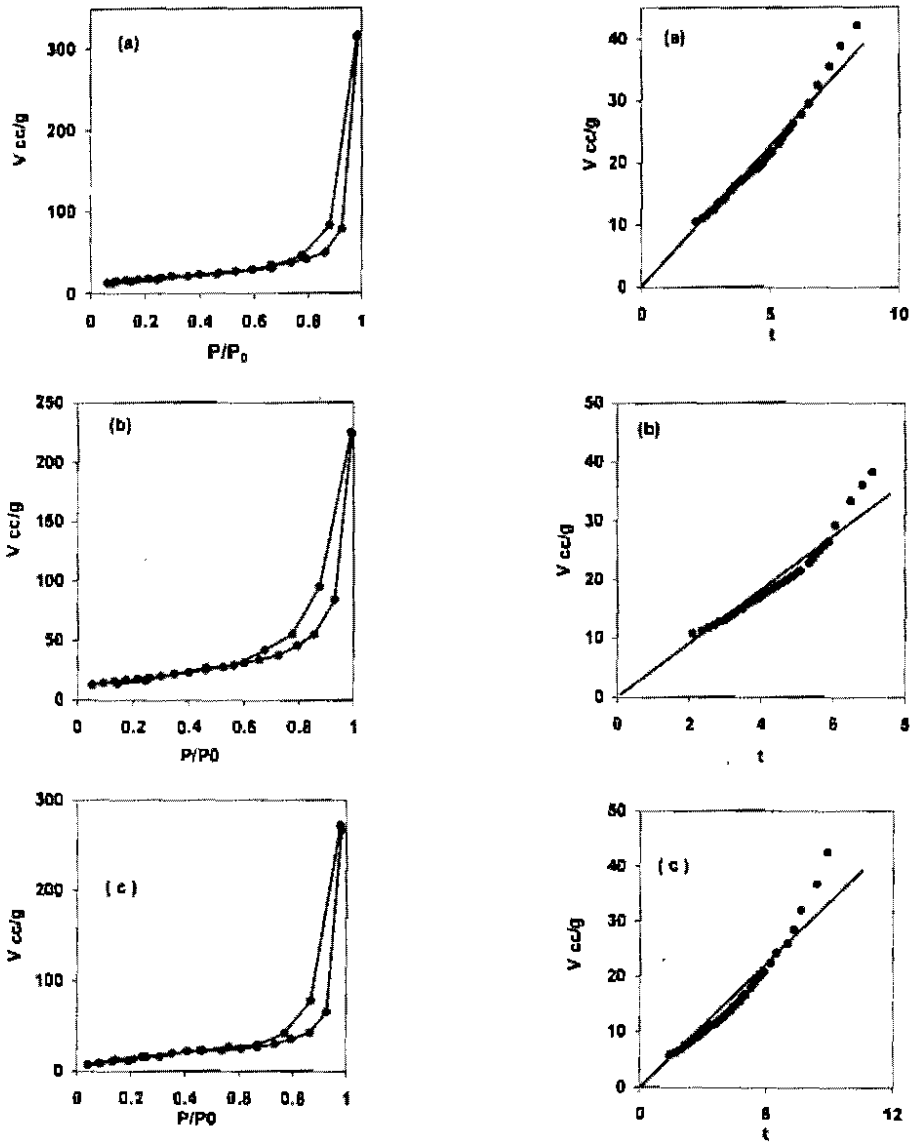

Fig. (4): Nitrogen adsorption isotherms and t- plots of; (a) Mg Al-LDH; (b) Cu-LDH; (c) Fe-LDH.

Table (2): The textural properties of prepared hydrotalcite- like samples.

Sample	S_{BET}	V_p cc/g	D_p (nm)
Mg Al- LDH	86.44	0.49	14.55
Mg Cu- LDH	61.61	0.34	14.3
Mg Fe- LDH	50.6	0.42	21.13

$D_p = 4\ V_{N2} / S_{BET}$.

These results are further corroborated by the pore size distribution (PSD) as shown in Fig .5. The PSD curves obtained from BJH formalism show a main contribution of pores with diameter close to ca 28 & 47 Å in all samples, however, the PSD curve for Cu-LDH is much broader and shifted to the right.

It is difficult to explain this modification that appears in the porosity features of LDH when a part of magnesium is substituted by copper and iron. The LDH layered structure with an interlayer free space (IFS) smaller than 3Å can not be responsible for any mesoporosity characteristics. The mesoporous structure of LDH may arise from interparticle space, hence, the mesopores characteristics could be defined by particle shape, size and also to the particles interconnection pattern. Consistently, pore formation in hydrotalcites is through interparticle packing, and the distribution of pores is influenced by the crystallite size and packing arrangement of crystallite **[Rives (2001)]**. In this view the mesopores features are the result of altering the microscopic morphology characteristics. However, one can assumes that the variation of the synthesis conditions (pH, the different nature of the ions present in synthesis medium, the different concentrations of the starting solutions) determined the changes of the microscopic morphology of copper and iron substituted samples. Similar results indicating significant modifications of the textural characteristics of hydrotalcite- like materials as a function of the synthesis conditions were previously reported by Malherbe et al. **[Malherbe, et al. (1997)]**.

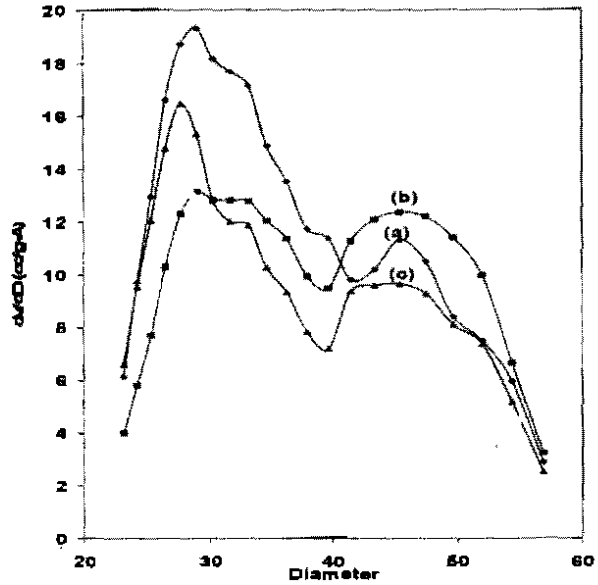

Fig. (5): PSD curves of ; (a) Mg Al-LDH; (b) Cu-LDH; (c) Fe-LDH.

The SEM images (Fig.6 (a)-(c)) show that all samples consist of intersected platelets of nearly hexagonal- shaped particles, interconnected with each other. However, overlapping of such platelets thereby exhibits a kind of spongy morphology.

Noteworthy, a different aspect emerged in the appearances. The differences are mainly due to the different mode of interconnection and agglomeration of the particles in the ternary LDH and also to the modification of the particle size. Interparticle space is larger for Cu-LDH (Fig.6 (b)).than for Fe- LDH or Mg Al- LDH., wider interparticle cavities developed in the iron substituted sample. This is presumably in accordance with the pore size distribution results wherein contributions of larger pores appear in greater numbers through interparticles for Cu-LDH.

The TEM images of the synthesized samples shows the presence of aggregates of well defined particles with hexagonal shape, characteristic for hydrotalcite- like materials **[Prinetto, et al. (2000)]**. A careful inspection of the images reveals that the particles themselves do not present any mesoporosity.

The SEM and TEM results further support the idea of the connection between the textural properties and the microscopic morphology of the samples.

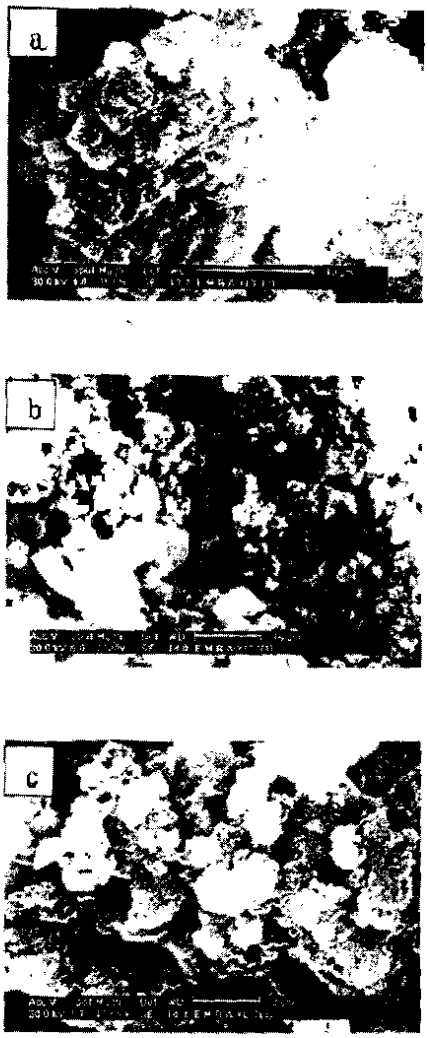

Fig.6: SEM micrographs of
(a) Mg Al-LDH; (b) Cu-LDH;
(c) Fe-LDH

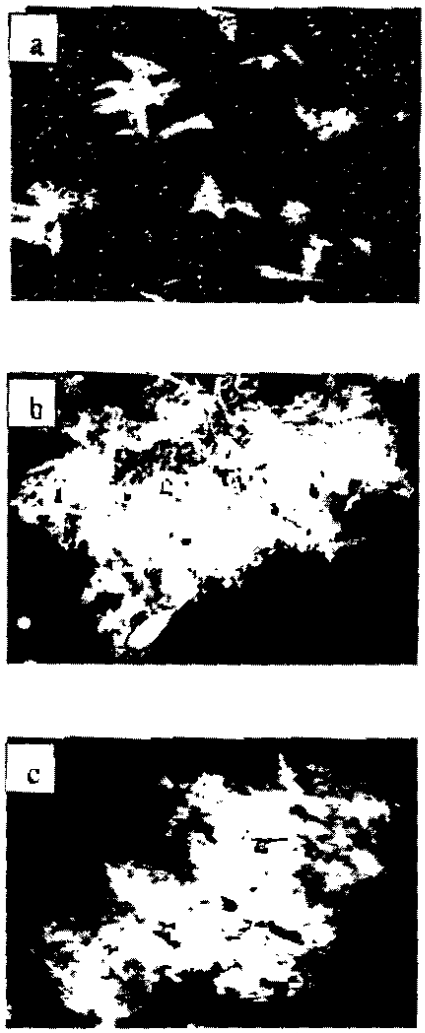

Fig.7: TEM micrographs of
(a) Mg Al-LDH; (b) Cu-LDH;
(c) Fe-LDH

CONCLUSION

The current study demonstrated that the porous structure for ternary layered double hydroxides (LDH) is significantly modified when copper or iron substituted LDH layer. Copper substituted-LDH presented a mesoporous structure with higher contribution of mesopores than Mg Al-LDH. while. iron substituted LDH developed the contribution of enlarged mesopores. Thus. the possibility of altering the textural

properties of LDH when a new metal is introduced in the layer may offer a new prospective in tailoring the textural characteristics of these materials for potential applications.

REFERENCES

Aramendia, M. A. Aviles, Y. Benitez, J. A. Borau, V. Jimenez, C. Marinas, J. M. Ruis, J. R. Urbano, F. J. Micropor. Mesopor. Mater. 29 (1999) 319.

Cavani, F. Trifiro, F. Vaccari, A. Catal. Today, 11 (1991) 173.

Crivello, M. Perez, C. Herrero, E. Ghione, G. Casuscelli, Castellon, E. R. Catal. Today 107-108 (2005) 215-222.

de Roy, A. Forano, C. EL Malki, K. Besse, J. B. in : M. L. Occelli, H. Robson (Eds.), Expanded clays and other microporous solids, synthesis of microporous materials. Van Nostrand Reinhold, New York, 1992, p. 108 (chapter 7).

Figueras, F. O. Top Catal. 29 (2004) 189.

Gregg, S.J Sing, K.S.W. Adsorption, Surface Area and Porosity, 2nd Edition, Acadimic Press, London, 1982.

Hernandez- Moreno, M. J. Ulibarri, M. A. Rendon, J. L. Serna, C. J. Phys. Chem. Miner. 12 (1985) 34.

Iglesias, A.H. Ferreira, O,A, Gouveia, D.X. Souza Filho, A. G. J. C. de Paiva, J. M. Filho, O.L. Alves. Journal of Solid State Chem., 178 (2005) 142-152.

Kannan, S. Dubey, A. Knozinger, H. J. Catal. 231 (2005) 381-392

Kannan, S. Swamy, C.S J Mater. Sci. 32, (1997) 1623.

Khan, A. I. Hare, D. O ' J. Mater. Chem. 12 (2002) 3191.

Khan, A. T. Lei, L. A. J. Norquist, D. O' Hare, Chem. Commun. 22 (2001) 2342.

Labajos, F. M. Rives, V. Ulibarri, M. A. J. Mater. Sci. 27 (1992) 1546.

Lazaridis, N. K. Pandi, T. A. Matis, K. A. Ind. Eng. Chem. Res. 43 (2004) 2209.

Malherbe. F. Forano. C. Besse. J.P. Microporous Mater. 10 (1997) 67.

Miyata, S. Clays Clay Miner. 23 (1975) 369.

Miyata, S. Clays clay miner. 31 (1983) 305.

Miyata, S. Okada, A. Clays Clay Miner. 44 (1977) 14.

Prinetto. F. Ghiotti. G. Graffin. P. Tchit. D. Micropor. Mesopor. 39(2000) 229.

Rives. Dubey. A. Kannan. S. Phys. Chem. Chem.. Phys.. 3 (2001) 4826.

Rives, V. Layered Double Hydroxides: Present and Future, Nova Sci. Pub. Inc. New York 2001.

Rives. V. Ulibarri. M. A. Coord. Chem. Rev., 181 (1999) 61.

Serna. C. J. White. J. L. Hem. S. L. Clays clay Miner. 25 (1977) 384.

Sing. K. S. W. Everrett, D. H. Haul. R. A. W. Moscou, L. Pierotti. R. Rouquerol, J. and Sieminiewska, T. Pure Appl. Chem., (1985), 57, 603.

Triforo, F. Vaccari, A. in: J. L. Atwood, J. E. D. Davies, D. D. Macnicol. F. Vogtle. J. M. Lehn, G. Alberti, T. Bein (Eds.). Comperhensive Supermolecular. Chemistry, Vol 7, Pergamon Elsevier Science. Oxford. 1996. p. 251.

Trujillano, R. Holgado, M. J. Gonzalez, J. L. Rives, V. Solid State Science 7 (2005) 931-935.

Vaccari, A. Appl. Clay Sci. 14(1999) 161.

Velu. S. Shah, N. Jyothi, T. M. Sivasanker, S. Micropor. Mesopor. Mater. 33(1999) 61.

Velu. S. Swamy. C. S. J. Mater. Sci. Lett. 15 (1996) 1674.

Vichi, F. M. Alves. O. L. J. Mater. Chem.7 (1997) 1631.

دراسة الخواص التركيبية للمواد ثنائية الطبقات الهيدروكسيلية وتأثير الأحلال الجزئى للماغنسيوم بكل من النحاس والحديد

لمياء سعد

تضمن هذا البحث تحضير مواد ثنائية الطبقات من الهيدروكسيدات مكونه من هيدروكسيدات الماغنسيوم والألومنيوم وأخرى تم إحلال الماغنسيوم جزئيا بكل من النحاس والحديد.

وقد تم تتبع التغير التركيبى للمواد المحضرة قبل عملية الأحلال وبعدها بأستخدام طرق التوصيف المختلفة مثل حيود الأشعة السينية (XRD)، التغيرات الناتجة عن المعاملات الحرارية (DTA & TGA)

التغير فى المساحة السطحية والمسامية (BET &MIP)، التغير فى التركيب النسيجى بأستخدام كل من الميكروسكوب النافذ والماسح (TEM &SEM)

وقد أثبتت الدراسة حدوث تغيرات إيجابية فى تركيب المواد المحضرة بعد عملية الأحلال الجزئى للماغنسيوم بكل من النحاس والحديد بما يفيد أستخدامها فى التفاعلات المختلفة.